Design and Testing of the 1.5 T Superconducting Solenoid for the BaBar Detector at PEP-II in SLAC

T.G. O'Connor , S. Shen, Lawrence Livermore National Laboratory, USA

P.Fabbricatore, S.Farinon, R.Musenich, C.Priano, INFN, Genova, ITALY

R.A.Bell, M.Berndt, .W.Burgess, W.Craddock , L. Keller, Stanford Linear Accelerator Center (SLAC), USA

O. Dormicchi, P. Moreschi, R.Penco, P.Valente, N.Valle, Ansaldo Energia, Genova Italy

Abstract — The 1.5 Tesla superconducting solenoid is part of the BABAR Detector located in the PEP-II B-Factory machine at the Stanford Linear Accelerator Center. The solenoid has a 2.8 m bore and is 3.7 m long. The two layer solenoid is wound with an aluminum stabilized conductor which is graded axially to produce a +/- 3% field uniformity in the tracking region. The 24 month fabrication, 3 month installation and 1 month commissioning of the solenoid were completed on time and budget. This paper summarizes the culmination of a 3 year design, fabrication and testing program of the BABAR superconducting solenoid. The work was completed by an international collaboration between Ansaldo, INFN, LLNL, and SLAC. Critical current measurements of the superconducting strand, cable and conductor, cool-down, operation with the thermo-siphon cooling, fast and slow discharges, and magnetic forces are discussed in detail.

I. INTRODUCTION

The magnet for the BABAR experiment at PEP-II in SLAC [1] is a thin superconducting solenoid within a hexagonal flux return. The nearly complete detector is shown in Fig 1, the solenoid is the cylinder just inside the flux return.

The design was based on criteria developed and tested over the last 15 years with detector magnets employing aluminum-stabilized thin solenoids [2]. The double layer coil is internally wound in a 35 mm thick 5083 aluminum support mandrel. Cooling pipes welded to the outside diameter of the support mandrel form part of the thermo-siphon system. Electrical insulation consists of dry wrap fiberglass cloth and epoxy vacuum impregnation. Table I shows the main parameters of the coil.

II CONDUCTOR

The conductor is composed of a superconducting Rutherford type cable embedded in a pure aluminum matrix through a co-extrusion process, which ensures good bonding between the aluminum and the superconductor.

In order to have a field homogeneity of +/- 3% in the large volume specified by the *BaBar* experiment, the current density in the winding is graded: lower in the central region and higher at the ends. The gradation is obtained by using conductor of two different thickness: 8.4 mm for the central region and 5 mm for the ends. Both 20 mm wide conductors are composed of a 16 strand Rutherford cable stabilized by pure aluminum.
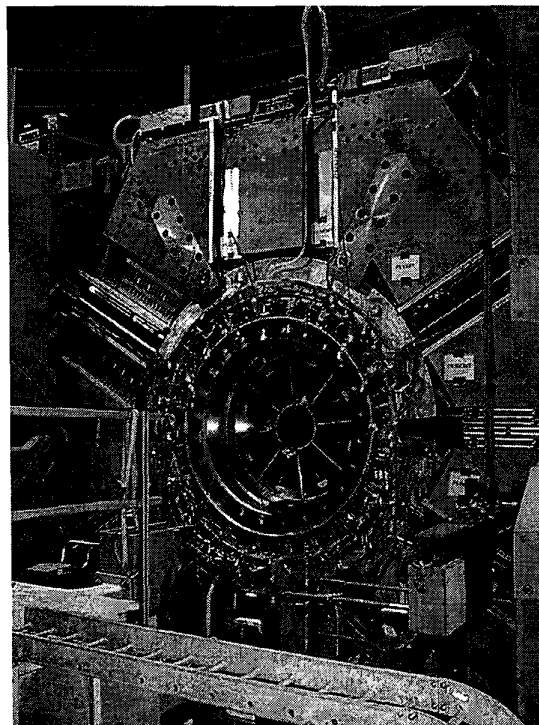
Fig. 1. View of BABAR solenoid in the hexagonal yoke

TABLE 1
MAIN CHARACTERISTICS OF BABAR SOLENOID (AS BUILT)

Central Induction	1.5T
Conductor peak field	2.3T
Winding structure	2 layers
	graded current density
Uniformity in the tracking region	± 3%
Winding axial length	3512 mm *at R.T*
Winding mean radius	1530 mm *at R.T.*
Operating current	4596 A (4650 A *)
Inductance	2.57 H (2.56 H *)
Stored Energy	27 MJ
Total turns	1067
Total length of conductor	10 300 m

(* Design value)

Table II describes the strands, the Rutherford cable and the final conductor characteristics as designed. Table III summarizes some characteristics of the conductors which were supplied by Europa Metalli (Fornaci di Barga –Italy). The co-extrusion processes were carried out at ALCATEL SWISS CABLE under assistance of ETH Zurich.

Critical current measurements were carried out on the Rutherford cables which were extracted from the pure aluminum matrix by chemical etching. The samples were arranged with the field normal to the wide face in order to reproduce the same field conditions experienced by the conductor inside the BaBar coil. The short samples were measured in the facility MA.RI.S.A., using the transformer method [3]. For each short sample critical current measurements were performed at different magnetic fields, see Fig. 2

The maximum field of 2.5 T was extrapolated from Fig. 2 and is listed in Table III. The critical current for all lengths is greater then the specified value: $Ic(B = 2.5\ T; T = 4.2\ K) = 12680\ A$.

In sample #3 the superconducting to normal transition was not observed, because the sample quenched before a significant voltage was measured. This was attributed to poor soldering of the sample within its holder. For this sample only, the quench current at different applied magnetic fields was measured. While sample #3 values listed in Table III are lower than the real critical currents, they are higher than those required by the critical current specifications (see Fig. 2).

III CONDUCTOR MARGINS

The peak field in the BaBar coil preliminary design, a single layer winding, was $B_{peak} = 2.5\ T$. At this field the critical temperature for NbTi is $T_C = 8.27\ K$. The current sharing temperature for this single layer design is 6.79 K. During the engineering design phase the coil configuration was modified from a single layer to a double layer design to increase the stability margin. This led to a reduction in the peak field of the thin conductor from 2.5 T to 2.3 T.

Using the packing factor of the completed coil the nominal current was found to be In= 4605 A. Since the field is higher in the inner layer, making this the more critical layer, the conductor margins were re-computed taking into account modifications to the peak field, critical current, and nominal current for these three sectors. The calculated values are listed in Table IV.

The highest I_n over I_c ratio for the thick conductor was, $I_n/I_c= 0.33$. The lowest current sharing temperature is the forward thin conductor, T_g =7.28 K. As a result of changing to a 2-layer design the coil has more temperature margin than the original single layer coil

TABLE II
SUMMARY OF SPECIFICATION FOR STRANDS, RUTHERFORD AND FULL CONDUCTOR

Component	Characteristic	Value
Strand	NbTi	Nb 46.5 +/- 1.5 wt % Ti
	Filament size	< 40 μm
	Twist pitch	25 mm
	Cu/NbTi ratio	> 1.1
	Cu RRR	Final >100
	Wire diameter	0.8 mm ± 0.005
Rutherford	Transposition pitch	< 90 mm
	Number of strands	16
	Final size	1.4 x 6.4 mm2
Conductor	Al-RRR	>1000
	Dimensions:	
	Thin conductor	(4.93 x 20)±0.02 mm
	Thick conductor	(8.49 x 20)±0.02 mm
	Rutherford-Al bonding	> 20 MPa
	Al/Cu/NbTi ratio:	
	Thin conductor	23.5:1.1:1
	Thick conductor	42.4:1.1:1
	Edge curvature radius	> 0.2 mm
	Critical current @ T=4.2 K; B=2.5 T	12680 A

TABLE III
RESULTS OF THE CRITICAL CURRENT TESTS.

Sample	Ic (B=2.5 T, T=4.2K)	N value
#1 thin	16800 A	27
#3 thick	15430 A	NA
#4 thin	15250 A	29
#5 thin	17660 A	40
#7 thick	14250 A	20
#9 thin	17810 A	36

TABLE IV
ELECTRICAL AND THERMAL MARGINS OF THE BABAR COIL AS CONSTRUCTED

Length	B_{peak} (T)	I_c (A) T=4.5 K, B= B_{peak}	I_n/I_c	T_g (K)
#5 inner layer thin forward	2.3	16550	28%	7.28
#7 inner layer thick middle	1.6	14220	33%	7.30
#9 inner layer thin backward	2.3	16950	27%	7.30

A parameter of interest is the enthalpy variation from 4.5 K to 7.28 K:

$$E_{u.v.} = \int_{4.5}^{7.28} Cp(T)\delta dT \qquad (1)$$

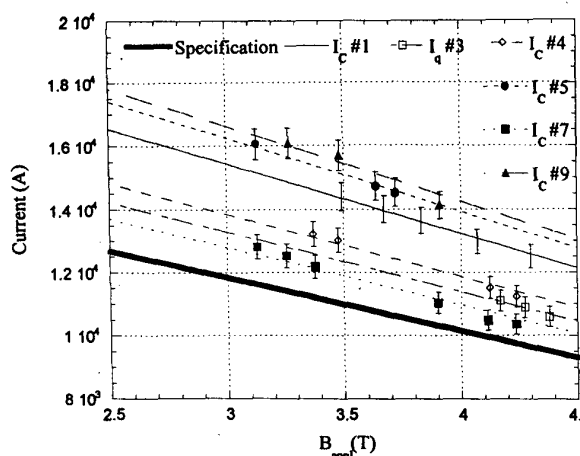where Cp(T) is the specific heat (in J/Kg) and δ the density.

Fig. 2, Critical current and quench currents vs. applied field [where applied field = external field plus the sample self field (B_{sf} = 0.68 Gauss/A)] performed on the six samples. The thick solid line represents the specification.

By averaging the thermal properties among the four components of the winding, aluminum, copper, NbTi and fiberglass epoxy, we find $E_{u.v.}$=3635 J/m^3. This enthalpy margin can be re-written in a more convenient way as energy per unit conductor length, resulting $E_{u.l.}$ = 0.36 J/m for thin conductor and $E_{u.l.}$ = 0.65 J/m for thick conductor. As comparison, ALEPH and CDF, two well known operational magnets, have an $E_{u.l.}$ 0.35 J/m and 0.1 J/m respectively.

IV. CRYOGENICS

The coil is indirectly cooled at an operating temperature of 4.5 K using the thermo-siphon technique. The liquid helium is circulated in channels welded to the support cylinder. The piping was designed for a steady-state cooling flow of 30 g/sec. The design heat loads are listed in Table V.

Cooldown and cryogenic supply to the coil and 40 K radiation shields is accomplished by a modified Linde TCF-200 liquefier/refrigerator.

Liquid helium and cold gas from the liquefier/refrigerator and its 4000 l storage dewar is supplied to the coil and shields via 60 m long, coaxial, return gas screened, flexible transfer line.

The schematic of the cooling system is shown in fig. 3.

It is possible to cool down the coil by a mixture of warm and cold He gas or by supplying colder and colder gas through the refrigerator. The shields are cooled by part of gas coming back from coil. The actual cool-down at SLAC took about a week as shown in fig.4

The heat load measurement at 4.5 K was performed by closing the input valve to the 4000 l control dewar and by measuring the LHe consumption in that dewar. This test gives pessimistic information because the transfer line losses are included too.

A total loss of 35 (+2, -3) W was measured, with no power in the coil. During the test the mass flow rate in each lead was 70 NLP/m, this means a load of 4 W per lead.
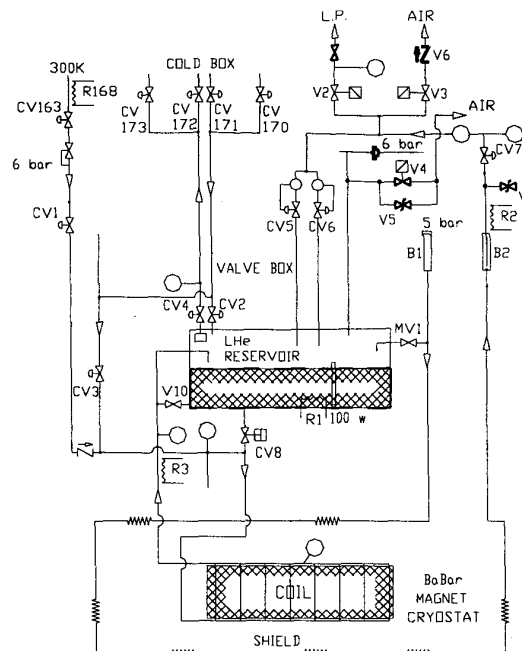

Fig. 3, Schematic of cryogenic circuit

When coil was powered at 1.58 T the mass flow rate per lead (at a voltage across each lead of 40 mV) was 90 NLP/m corresponding to a heat load of 5 W per lead. Mixing these data and considering that 3 W loss can be due to the transfer line we can assume that heat load is between 19 W and 24 W + 14 l/h. This very low value of the loss is partially due to the shield temperature (45 K as shown later).
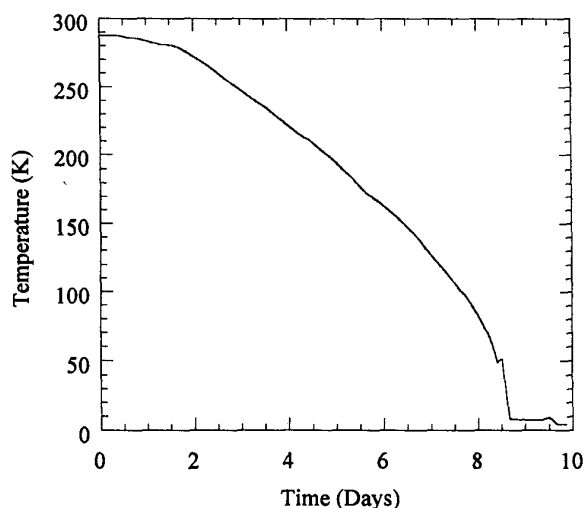

Fig. 4, Coil average temperature during cool-down

The shields were cooled by cool helium gas coming from the LHe reservoir in the Valve Box. The shield temperatures range between 37 and 49K with a mass flow rate of 0.35 g/s. Since the enthalpy variation of helium gas at atmospheric pressure between 4.5 and 45 K(average shield temperature) is about 250 J/g, the total load at the shield is 87 W.

TABLE V
DESIGN SOLENOID CRYOGENIC HEAT LOADS

Item	Liquefaction g/s (l/h)	Refrigeration at 4.4K (Watts)	Liquid Nitrogen at 77 K (Watts)
Current Leads	0.42 (12)		
Solenoid Radiation and Conduction Heat Load and Valve box Heat Load		70	
Solenoid Heat Shield Heat Load			350
Total Steady State Load	0.42 (12)	70	350

V. OPERATION

The coil current was incrementally increased to 4605 A. The central field measured with an Hall probe was 1.503 T. The operating current for 1.50 T was then determined to be 4596 A and the design current (1.05 times the nominal current) was determined to be 4825 A.

On charging the coil at 1.00 A/s the inductive voltage across the coil was 2.573V. The measured inductance is 2.573 H, which is in good agreement with computation (2.56 H).

The final step in the commissioning process was to charge the solenoid to the design current of 4826 A. The measured field at the design current was 1.58 T.

During these tests two fast discharges occurred due to false trigger of the Quench Detector System. This problem was fixed by modifying the front end electronics of the quench detection system (QDS).

VI. FAST AND SLOW DISCHARGE

The coil is protected with the usual method of a resistor in parallel. If a quench is detected (50 mV unbalance signal between the two voltages in two layers), a breaker opens, closing the current in coil and dump resistor. The peak voltage at the coil ends can be as high as 340V. Considering that the center tap of the dump resistor was shorted to ground, the maximum voltage to ground is 170 V.

Fig. 5 and 6 show current and voltage during a fast dump

from 4600 A. The voltage signal from each layer is plotted in Fig 6.

The fast discharge from the nominal current causes a quench due the heating of the supporting cylinder (Quench Back). The coil temperature increases to 37 K uniformly. In these conditions about 5 hours are needed to cool-down the coil again, fill the reservoir and be ready for re-charging.
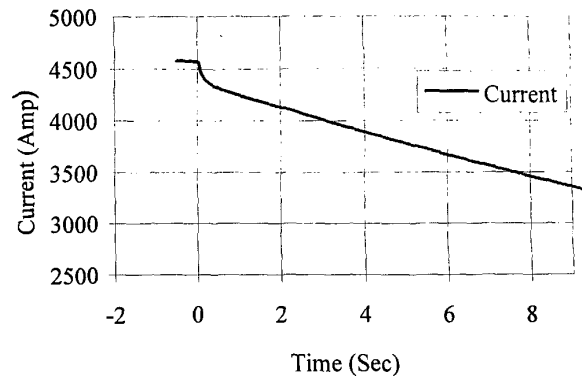

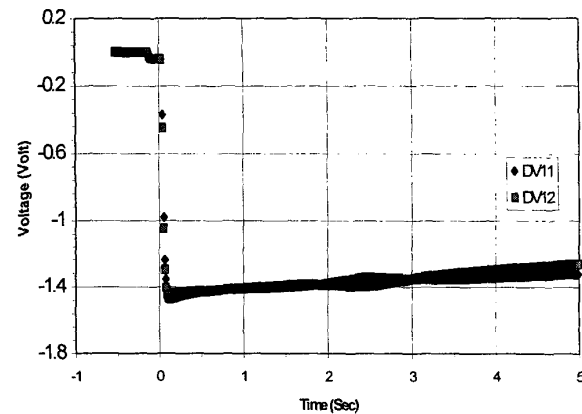Fig. 5, Coil current during fast discharge. Time t=0 is the breaker opening

Fig. 6, Attenuated voltages at two coil layers during fast discharge

VII. MAGNETIC FORCES

The coil is placed inside a non-symmetric flux return yoke. This gives rise to axial offset forces. In order to have an offset force in one direction only (no inversion during the ramp up), the coil was positioned with 30 mm axial displacement in the forward direction. Fig. 7 shows the axial offset force as resulted from the strains in the three Inconel 718 tie rods placed at the backward side. These tie rods were designed to hold forces as high as 25 ton with a safety factor of 4

Forces on single tie rod and total force (sum of the three) are shown. The total force is forward directed and has a maximum of 8 ton at 3800 A. The three tie rods at the opposite side (forward) are not strained.

The force behavior vs. current is in agreement with a axial displacement of 33 mm in forward direction of the coil with

respect to the iron (as resulted from ANSYS and MERMAID 2D computation). When positioning the coil, the aim was to set the displacement to 30 mm in order to have a maximum force at 2500 A and a few tons at full current. The offset force is not equally shared by the three tie rods due to misalignment of the coil in the flux return.

The average strain in the three tie rods is 500 μm corresponding to 0.3 mm displacement. The displacement measured with mechanical probes gave 1 mm axial displacement. This could be due to the spring washers on tie rods, causing a displacement not resulting as stress on tie rods.
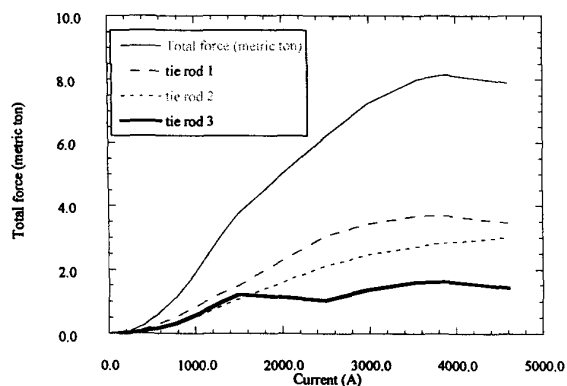

Fig. 7, Axial forces in the solenoid backward end tie rods.

Fig. 8 shows the net axial force on the coil versus the fraction of nominal current. The lines with boxes and triangles are calculations using the MERMAID 2D code [4] and ANSYS respectively, while the diamonds are measurements using strain gauges attached to the axial tie rods.
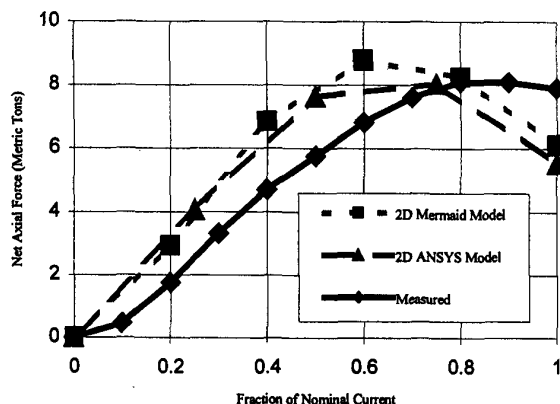
The net axial force is the difference of two large compressive forces of approximately 380 metric tons on the forward and backward ends of the coil. It is very sensitive to the axial location of the coil within the barrel; the gradient is approximately 1.5 metric-ton/mm of axial displacement. Even though the shapes of the measured and calculated curves are somewhat different, the agreement is

remarkably good considering the uncertainty in the location of the coil and the magnet model.

The coil would have to be moved in the backward direction from 32-33 mm to 30 mm to reduce the force at full current to the design value. The present location of the coil yields axial forces which are within the margin of the tie-rod force limits and therefore, don't require moving the axial location of the coil within the flux return.

VIII. SUMMARY

The superconducting solenoid was successfully commissioned in March 1998, and following a detailed field map the solenoid was then warmed up for final assembly of the BABAR detector. The solenoid will be operational again in November 1998

IX. ACKNOWLEDGMENTS

We wish to thank all concerned who contributed to the design, tests, analysis and graphics contained in this paper.

REFERENCES

[1] BABAR collaboration 'Technical design report," *SLAC note R-95-457*, 1995
[2] H.Desportes et al, 'Construction and Test of the CELLO Thin-Wall Solenoid' *Ad. Cryogenic Eng.* 25, p. 175, 1980
[3] P.Fabbricatore, R.Musenich, and R.Parodi, "Inductive method for critical measurement of superconducting cables for high energy physics applications," NIM, vol. A302, 1991, pp. 27-35
[4] Program MERMAID was written at the Budker Institute of Physics, Novosibirsk, 1994.

Fig. 8, Net axial force on the superconducting solenoid vs. fractional current. Positive force is in the forward direction. Coil offset = 32 mm in the forward direction. The bucking coil current = 0 Amps.